Photochemical & Photobiological Sciences

RSC Publishing

PAPER

# Effect of nanocavities on the torsional dynamics of thioflavin T in various non-aqueous reverse micelles†

Cite this: *Photochem. Photobiol. Sci.*, 2013, **12**, 369

Aninda Chatterjee and Debabrata Seth*

The photophysics of thioflavin T (ThT) were observed in different non-aqueous reverse micelles by using steady state absorption and emission spectroscopy and time resolved fluorescence spectroscopy. We have used glycerol, ethylene glycol, dimethyl formamide, methanol and acetonitrile as polar solvents to form reverse micelles. In all reverse micelles with increase in *w* (*w* = [polar solvent]/[AOT]) the fluorescence quantum yield decreased in a regular way. The time resolved fluorescence study of ThT in different reverse micelles shows the similar trend as like above. We had plotted a calibration curve using the fluorescence quantum yield of ThT in glycerol–methanol mixtures *vs.* viscosity and from that curve we found that ThT faced a greater microviscosity in glycerol pool of AOT/isooctane/glycerol reverse micelles than in the pure glycerol, even at the highest *w* value. In all reverse micelles the emission quantum yield of ThT was retarded several times compared to neat solvents. We have found that the fluorescence quantum yield of ThT decreased with gradual increase in polarity by studying the emission properties of ThT in dioxane–water mixtures of different polarity.

Received 13th June 2012,
Accepted 27th September 2012

DOI: 10.1039/c2pp25297j

**www.rsc.org/pps**

## 1. Introduction

Thioflavin-T (ThT) is a very important dye molecule which forms highly fluorescent complexes with amyloid like fibrils. It binds with amyloid fibrils with subsequent changes in its fluorescence properties. These changes in fluorescence properties are widely used for studying the formation of amyloid fibrils *in vitro* and hence ThT is widely used to study several neurodegenerative disorders, such as Alzheimer's disease, Parkinson's disease *etc.*[1,2] The formation and deposition of amyloid fibrils, insoluble filamentous protein aggregates, in different organism tissues are generally responsible for above mentioned neurodegenerative disorders and several other diseases, such as cataracts, type II diabetes *etc.*

ThT (Scheme 1) undergoes photoinduced twisted intramolecular charge transfer (TICT) in the excited state by the ultra fast torsional relaxation of the aromatic rings through the C–C bond and this torsional motion is responsible for the fluorescence quenching process and hence the extremely low quantum yield in solutions of low viscosity.[3,4] The increase in quantum yield of ThT when bound to amyloid fibrils is due to the inhibition of rotation of the two rings along the C–C bond.[3,4] The binding of ThT to amyloid fibrils may be either monomeric, dimeric or micellar.[5,6] Groenning *et al.* had performed the isothermal titration calorimetry experiments of ThT binding to fibrils and found that the free energy of this binding is dominated by entropy indicating that electrostatic interaction has hardly any effect on binding.[7] Khurana *et al.*, using atomic force microscopy, examined the topography of amyloid fibrils in the presence of ThT and found that at 20 μM concentration showed "bumps", which were considered as the micelles bound to the surface of the fibrils.[8] Later this micelle hypothesis has been opposed by the fact that the critical micelle concentration (CMC) of ThT was found to be 31.4 ± 5.2 μM by fluorescence anisotropy measurement rather than 4 μM.[8,9] Singh *et al.* using TRANES (time-resolved area normalized emission spectra) has shown that the TICT state of ThT is emissive in nature.[10]

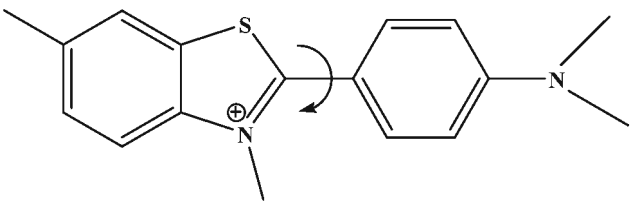


**Scheme 1** A schematic representation of the thioflavin T cation.

The spectroscopic and photophysical properties of ThT were studied in different restricted and confined media, such as micelles, reverse micelles, cyclodextrins and also in DNA.[11–15] Ilanchelian and Ramaraj studied the spectroscopic properties of ThT in DNA and reported both the electrostatic

*Department of Chemistry, Indian Institute of Technology, Patna 800013, Bihar, India. E-mail: debabrata@iitp.ac.in; Fax: +91-612-2277383*

†Electronic supplementary information (ESI) available. See DOI: 10.1039/c2pp25297j

and groove binding interaction between ThT and DNA. They showed that addition of NaCl to the system was responsible for weakening of the electrostatic interaction in between ThT and DNA.[12]

Quantum chemical calculations on the ThT cation shows that the presence of a methyl group on the nitrogen of benzthiazole ring prevents the molecule adopting the planar configuration. When the two aromatic rings are in perpendicular positions the conjugation between the Π electron clouds of the two aromatic rings breaks down and the two moieties behave as independent chromophores. These calculations also showed that in the ground state the positive charge of the entire ThT cation mostly resides on the benzthiazole ring of the cation and the amount of positive charge gradually increases with the increase of torsion angle in between the benzthiazole ring and the dimethylaniline rings and reaches maximum at torsion angle 90°. The opposite thing is found to happen on excitation of the molecule from the ground $S_0$ state to the $S_1$ state *i.e.* in the excited state the dimethylaniline ring contains a higher amount of positive charge and this amount also gradually increases with the increase of torsion angle between the two aromatic rings.[1,16,17] Amdursky *et al.* studied temperature dependence of the fluorescence properties of thioflavin-T in propanol.[18]

AOT/oil/water reverse micelles are known to provide a confined water pool. The size of this confined water pool depends on the $w_0$ value, where $w_0$ = [water]/[AOT]. The nature of the nanoconfined water is quite different than the bulk water. Singh *et al.*[15] studied the photophysical properties of ThT in AOT/heptane/water reverse micelles and found that the nanoconfined water pool was responsible for the 250 fold increase of the fluorescence quantum yield from that in the bulk water. They showed that with a gradual increase in the pool size the fluorescence quantum yield and the fluorescence lifetime decreased nonlinearly. They used both steady state and femtosecond fluorescence upconversion techniques to study the dynamics of ThT. It is reported in the literature that other polar solvents, such as methanol, acetonitrile, glycerol, DMF, formamide, ethylene glycol, can be used for preparing reverse micelles of different $w$ ($w$ = [polar solvents]/[AOT]) values. These non-aqueous reverse micelles are of great importance and interest. In 1984 Friberg and Podzimek first studied the formation of ethylene glycol microemulsion by using ethylene glycol and lecithin and decane.[19] Methanol, acetonitrile, DMF, formamide, glycerol and ethylene glycol are the most commonly used polar solvents to form non-aqueous reverse micelles. Falcone *et al.*[20] studied the properties of non-aqueous reverse micelles using six polar solvents, such as glycerol, ethylene glycol, propylene glycol, formamide, dimethyl formamide, dimethylacetamide. They compared these reverse micelles with the aqueous reverse micelles using the solvatochromic behaviour of 1-methyl-8-oxyquinolinium betaine dye. Laia *et al.*[21] studied the nature of the microemulsions with trapped polar non-aqueous solvents (glycerol, ethylene glycol, formamide) inside the core using the dynamic light scattering (DLS) method. They reported the formation of clusters between these microemulsion droplets by means of attractive interactions between them. The highest attractive interaction was observed in the case of formamide and the lowest in the case of glycerol.[21] The solvation dynamics of methanol and acetonitrile in AOT/heptane/methanol and AOT/heptane/acetonitrile reverse micelles were studied.[22–26] In this work we have studied the photophysical process of ThT molecules in the non-aqueous reverse micelles to study the effect of confinement in the solvent pool of the microemulsions. In this study methanol–glycerol mixtures are employed as the medium in order to see the effect of viscosity of the medium, and dioxane–water mixture as the medium to see the effect of polarity on the exited state properties of ThT.

## 2. Materials and method

Thioflavin T was purchased from Sigma-Aldrich as its chloride salt and used after twice recrystallizing from a 3 : 1 mixture of acetonitrile and ethanol, as described in the literature.[27] Dioctyl sodium sulfosuccinate or Aerosol OT (AOT), was purchased from Sigma-Aldrich. Methanol, isooctane and 1,4 dioxane (spectroscopic grade) were purchased from Spectrochem, India. Acetonitrile (spectroscopic grade) was purchased from SRL, India. Glycerol (ACS grade) and DMF (HPLC grade) were purchased from RANKEM, India. Ethylene glycol was purchased from CDH, India. AOT was dried in vacuum and used as described in the literature.[15] The concentration of AOT maintained in all measurements is 0.1 (M).

The ground state UV-Vis absorption measurements were carried out using UV-Vis spectrophotometer (Model: UV-2550, SHIMADZU). The steady state fluorescence emission measurements were done using Fluoromax-4P spectrofluorometer (HORIBA JOBIN YVON). The fluorescence quantum yield of ThT in different media was calculated using the fluorescence quantum yield of Coumarin 480 in water ($\phi_f$ = 0.66)[28] as a reference by using the following equation:

$$\phi_s = \phi_r \frac{I_s A_r n_s^2}{I_r A_s n_r^2} \quad (1)$$

where subscript s and r stand for the sample and reference, respectively, and $I$ stands for the integrated area under the emission band, $A$ stands for the absorbance of the solution at the excitation wavelength and $n$ stands for the refractive index of the solvent. The steady state emission spectra was fitted by the "log normal line shape function" which is defined as

$$I(\nu) = I_0 \exp\left[-\ln 2\left(\frac{\ln[1 + 2b(\nu - \nu_p)/\Delta]}{b}\right)^2\right] \quad (2)$$

where $\nu_p$, $I_0$, $\Delta$ and $b$ are the peak position, amplitude, width and asymmetry parameter, respectively. For steady state fluorescence and absorption measurement the temperature was kept constant at 298 K by using a Jeiotech refrigerated bath circulator (Model: RW0525G).

 

The fluorescence transients were taken with the use of the picosecond-resolved time-correlated single-photon counting (TCSPC) technique. We used a time-resolved fluorescence spectrophotometer from Edinburgh Instruments (Model: LifeSpec-II, UK) and we used a picosecond diode laser at 405 nm as an excitation source. The instrument response function (IRF) of our system is 75 ps. The fluorescence transients were detected at magic angle (54.7°) polarization using a Hamamatsu MCP PMT (3809U) as a detector. The decays were analysed using F-900 decay analysis software. The observed fluorescence transients were fitted after deconvoluting IRF by using the following equation:

$$I(t) = A + \sum_{i=1}^{N} B_i \exp\left(-\frac{t}{\tau_i}\right) \quad (3)$$

where $B_i$ is the pre-exponential factor with the characteristic lifetime $\tau_i$ and $A$ is the background. The amplitude weighted average lifetime was calculate as $\langle\tau\rangle = \sum_{i=1}^{N} (C_i\tau_i)$, where $C_i = \frac{B_i}{\sum_{i=1}^{N} B_i}$.

All experiments were carried out three times to check the reproducibility of the data.

The fluorescence anisotropy decays ($r(t)$) were measured by using the same instrument (Model: LifeSpec-II). For the anisotropy measurement, the emission intensities at parallel ($I_{||}$) and perpendicular ($I_{\perp}$) polarizations were alternatively collected by fixing the time for both the decays. Motorised polarizers were used to collect the parallel and perpendicular decays. Then the following equation was used to get the $r(t)$.

$$r(t) = \frac{I_{||}(t) - GI_{\perp}(t)}{I_{||}(t) + 2GI_{\perp}(t)} \quad (4)$$

$G$ is the correction factor for detector sensitivity to the polarization direction of the emission. The F-900 software was used to fit the anisotropy decay. For time resolved measurement temperature was kept constant at 298 K by using peltier-controlled cuvette holders from Quantum Northwest (Model: TLC-50).

## 3. Results and discussion

### 3.1 Steady state absorption and emission study

The absorption maxima of ThT in different neat solvents, such as water, methanol (MeOH), acetonitrile (ACN), dimethyl formamide (DMF), ethylene glycol (EG) and glycerol (Gly), are found at 411, 415, 415, 417, 421 and 423 nm, respectively. In isooctane–AOT mixture the absorption maximum of ThT was found at 24 096 $cm^{-1}$ (415 nm). In isooctane/AOT/MeOH reverse micelles with gradual addition of methanol the absorption maxima of ThT showed blue shift. At $w$ = 8 the absorption maxima was found at 24 390 $cm^{-1}$ (410 nm) as shown in Fig. 1a. In isooctane/AOT/DMF reverse micelles we have observed a similar feature. With increase in $w$ value, the absorption maximum of ThT showed a blue shift. At $w$ = 3 the absorption maxima was found at 24 330 $cm^{-1}$ (411 nm), as shown in Fig. 1b. In isooctane/AOT/EG reverse micelles the absorption maxima of ThT showed red shift as shown in Fig. 2a. In isooctane/AOT/Gly reverse micelles the absorption maximum of ThT gradually red shifted with an increase in $w$ value (Fig. 2b). In isooctane/AOT/ACN reverse micelles the absorption peak remains almost unchanged with addition of ACN in the isooctane–AOT mixture. ThT is a cationic probe and the surfactant AOT is an anionic molecule, therefore certainly some electrostatic interaction between ThT and AOT is possible. In SDS micelles Kumar *et al.*[14] found a red shift in the absorption maximum of ThT. In isooctane/AOT/water reverse micelles Singh *et al.*[15] found a red shift in the absorption maximum of ThT. These bathochromic shifts are due to the electrostatic interaction between the cationic ThT and the anionic head group of the surfactant.[14,15] A ThT molecule undergoes a red shift in the absorption spectral peak when it faces a less polar environment.[29] In our case we have observed a blue shift in the absorption peak of ThT in the non-aqueous polar solvent containing reverse micelles except for Gly- and

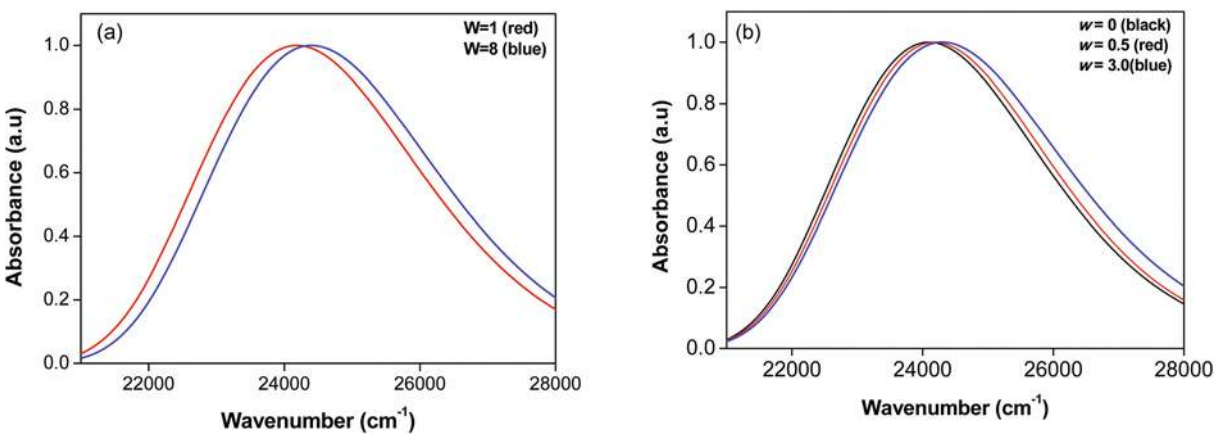


**Fig. 1** The spectral shift in absorption spectra of ThT in (**a**) isooctane/AOT/MeOH reverses micelles, (**b**) isooctane/AOT/DMF reverses micelles of different $w$ values.

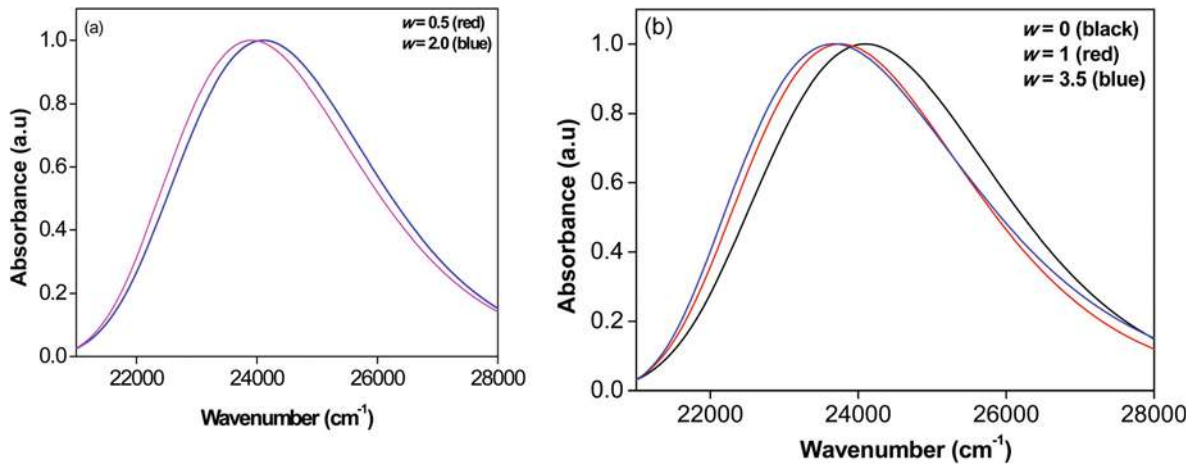


**Fig. 2** The spectral shifts in absorption spectra of ThT in (**a**) isooctane/AOT/EG reverse micelles, (**b**) isooctane/AOT/Gly reverse micelles of different *w* values.

EG-containing reverse micelles. The blue shift of the absorption peak is also reported in the literature.[30] In isooctane/AOT/DMF reverse micelles the sodium counter ion disrupts the intermolecular structure of DMF and as a result the weak intermolecular interaction between the DMF molecules breaks down, thereby highly solvating the $Na^+$ counter ion. As a result, the naked polar sulfonate head groups of AOT become available for electrostatic binding with the ThT cation. An increase in DMF in the polar core of reverse micelle causes more and more $Na^+$ ions to become solvated and hence more and more polar head groups of AOT become free for electrostatic binding between the $ThT^+$ and the negatively charged sulfonate head group. This electrostatic interaction causes the ground state of the molecule to be sufficiently stabilised compared to the excited state, as this complex formation by electrostatic interaction is a ground state phenomenon, and hence the absorption spectra of ThT in this isooctane/AOT/DMF undergoes a blue shift. The $Na^+$ counter ion undergoes electrostatic binding with the AOT polar head group and competes with the ThT cation. When $Na^+$ ions are removed from the sulfonate group by solvation, the ThT cation gets enough advantage to form electrostatic binding. This may be the probable reason for the blue shift of the absorption peak of ThT. A similar kind of blue shift in the absorption spectra of 1-methyl-8-oxyquinolinium betaine (QB) dye was reported in the literature.[20] In the case of isooctane/AOT/MeOH reverse micelles, gradual addition of methanol to the polar core of the reverse micelle causes the solvation of the polar head group of the AOT (sulfonate head group) by means of hydrogen bonding.[31] This solvation results in the weakening of the electrostatic interaction between the cations (both $Na^+$ and $ThT^+$) and the anionic head group of AOT. So the interaction between the ThT cation and the AOT becomes weak with gradual increase in *w* value and it may be possible that the free ThT cation starts to get solvated by free methanol (*i.e.* the methanol molecules not solvating the polar head group of the AOT). This may be the probable explanation of the blue shift of the absorption peak of ThT in this reverse micelle. In the case of Gly- and EG-containing reverse micelles the addition of these two polar liquids in the isooctane–AOT mixture causes the weakening of the electrostatic interaction between the $SO_3^-$ polar head group of AOT and the ThT cation. As a result the cationic dye molecule moves towards the polar core from the interface with a gradual increase in *w* value. So the absorption peak in both these reverse micelles undergoes a red shift with a gradual increase in *w* value. In all reverse micelles (except for glycerol containing reverse micelles) the absorption peak of ThT is blue shifted compared to that in the respective neat polar solvents. Even at the highest *w* value the absorption peak of ThT is blue shifted compared to the bulk solvents. These data showed that the ThT is facing a less polar environment inside the reverse micelles compared to the bulk solvents.

The fluorescence emission maxima of ThT in different neat solvents, such as MeOH, ACN, DMF, EG and Gly, are found at 478, 479, 485, 487 and 485 nm, respectively. In the isooctane–AOT mixture the emission maximum of ThT was found at 475 nm. In isooctane/AOT/MeOH reverse micelles we have observed little red shift in the emission maxima of ThT with gradual addition of methanol and the fluorescence intensity gradually decreases, as shown in Fig. 3a. In isooctane/AOT/ACN and isooctane/AOT/DMF reverse micelles we have observed a small red shift in the emission maximum of ThT and the fluorescence intensity gradually decreased with increase in *w* value. Similarly in isooctane/AOT/EG (Fig. 3b) and isooctane/AOT/Gly reverse micelles (Fig. 3c) we have observed a red shift in emission maximum of ThT and the fluorescence emission intensity gradually decreased with a gradual increase in *w* value. In all reverse micelles we have observed a blue shift in the emission spectra compared to neat solvent.

The emission quantum yield of ThT in different reverse micelles have been measured and tabulated in Table 1. In isooctane/AOT/MeOH reverse micelles the emission quantum yield ($\phi_f$) of ThT at $w = 1$ is 0.030 and in neat MeOH the quantum yield of ThT is ~0.0005. Therefore the quantum yield of ThT increases ~60 times in methanol containing reverse

 

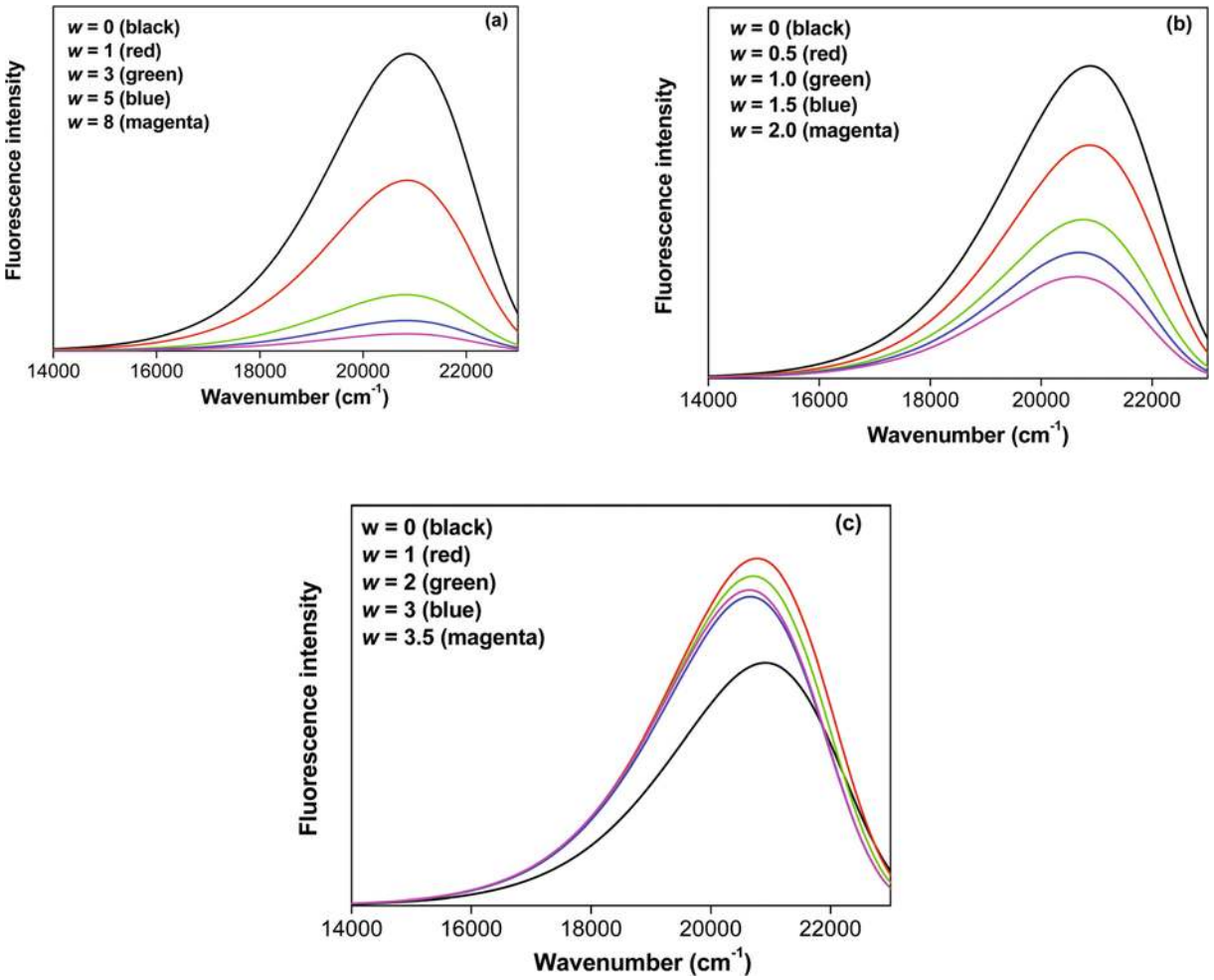


**Fig. 3** The changes in emission spectra of ThT in (**a**) isooctane/AOT/MeOH reverse micelles, (**b**) isooctane/AOT/EG reverse micelles and (**c**) isooctane/AOT/Gly reverse micelles of different *w* values.

**Table 1** The absorption and emission maximum and lifetime of ThT in isooctane/AOT/polar solvents reverse micelles (RM) of different *w* ([polar solvents]/[AOT]) values

| No. | System | $\phi_f$ | $\tau_f$ [a] (ns) | $k_r$ ($s^{-1}$)[b] ($\times 10^9$) | $1/\tau_F = k_r + k_{nr}$ ($\times 10^9$) ($s^{-1}$) | $k_{nr}$ ($\times 10^9$) ($s^{-1}$) | $\lambda_{max}$ (abs) $cm^{-1}$ (nm) | $\lambda_{max}$ (em) $cm^{-1}$ (nm) |
|---|---|---|---|---|---|---|---|---|
| 1 | AOT–isooctane mixture | 0.06 | 0.462 | 0.130 | 2.164 | 2.03 | 24 096 (415) | 20 906 (475) |
| 2 | Gly RM at $w = 1$ | 0.112 | 0.639 | 0.175 | 1.565 | 1.39 | 23 696 (422) | 20 772 (478) |
| 3 | Gly RM at $w = 2$ | 0.105 | 0.593 | 0.177 | 1.686 | 1.51 | 23 696 (422) | 20 705 (479) |
| 4 | Gly RM at $w = 3$ | 0.096 | 0.556 | 0.173 | 1.798 | 1.63 | 23 696 (422) | 20 657 (481) |
| 5 | Gly RM at $w = 3.5$ | 0.096 | 0.560 | 0.171 | 1.785 | 1.61 | 23 640 (423) | 20 644 (481) |
| 6 | EG RM at $w = 0.5$ | 0.046 | 0.317 | 0.145 | 3.155 | 3.01 | 24 096 (415) | 20 868 (476) |
| 7 | EG RM at $w = 1.0$ | 0.031 | 0.214 | 0.145 | 4.673 | 4.53 | 24 038 (416) | 20 755 (478) |
| 8 | EG RM at $w = 1.5$ | 0.024 | 0.166 | 0.144 | 6.024 | 5.88 | 23 923 (418) | 20 689 (480) |
| 9 | EG RM at $w = 2.0$ | 0.02 | 0.143 | 0.140 | 6.993 | 6.85 | 23 923 (418) | 20 638 (481) |
| 10 | DMF RM at $w = 0.5$ | 0.058 | 0.334 | 0.174 | 2.99 | 2.82 | 24 213 (413) | 20 859 (476) |
| 11 | DMF RM at $w = 1.0$ | 0.045 | 0.278 | 0.162 | 3.60 | 3.43 | 24 271 (412) | 20 825 (476) |
| 12 | DMF RM at $w = 2.0$ | 0.028 | 0.185 | 0.151 | 5.405 | 5.25 | 24 271 (412) | 20 768 (478) |
| 13 | DMF RM at $w = 3.0$ | 0.018 | 0.126 | 0.143 | 7.940 | 7.79 | 24 330 (411) | 20 704 (479) |
| 14 | ACN RM at $w = 1.0$ | 0.044 | 0.333 | 0.132 | 3.003 | 2.87 | 24 096 (415) | 20 839 (476) |
| 15 | ACN RM at $w = 3.0$ | 0.025 | 0.208 | 0.120 | 4.807 | 4.69 | 24 096 (415) | 20 778 (478) |
| 16 | ACN RM at $w = 5.0$ | 0.016 | 0.103 | 0.155 | 9.708 | 9.55 | 24 154 (414) | 20 741 (479) |
| 17 | MeOH RM at $w = 1.0$ | 0.030 | 0.277 | 0.108 | 3.610 | 3.50 | 24 213 (413) | 20 854 (476) |
| 18 | MeOH RM at $w = 3.0$ | 0.01 | 0.101 | 0.099 | 9.901 | 9.80 | 24 390 (410) | 20 816 (477) |
| 19 | MeOH RM at $w = 5.0$ | 0.006 | 0.057 | 0.105 | 17.543 | 17.44 | 24 390 (410) | 20 818 (477) |
| 20 | MeOH RM at $w = 8.0$ | 0.003 | 0.040 | 0.075 | 25.00 | 24.92 | 24 390 (410) | 20 815 (477) |

[a] $\tau_f = a_1\tau_1 + a_2\tau_2 + a_3\tau_3$. [b] $k_r = \phi_f/\tau_f$.

micelles compared to that in neat methanol due to confinement of ThT in the polar core of the reverse micelles. With an increase in $w$ value $\phi_f$ gradually decreases, at $w$ = 8, $\phi_f$ of ThT becomes 0.003. In isooctane/AOT/ACN reverse micelles the emission quantum yields ($\phi_f$) of ThT at $w$ = 1 is 0.044, and in neat ACN the quantum yield of ThT is ~0.0003. Therefore the quantum yield of ThT increases ~147 times in ACN containing reverse micelles compared to that in neat ACN. With increasing $w$ value $\phi_f$ gradually decreases, at $w$ = 5, $\phi_f$ of ThT becomes 0.016. In isooctane/AOT/DMF reverse micelles the emission quantum yields ($\phi_f$) of ThT at $w$ = 0.5 is 0.058, and in neat DMF the quantum yield of ThT is ~0.0007. Therefore the quantum yield of ThT increases ~83 times in DMF containing reverse micelles compared to that in neat DMF. With an increase in $w$ value $\phi_f$ gradually decreases, at $w$ = 3, $\phi_f$ of ThT become 0.018. In isooctane/AOT/EG reverse micelles the emission quantum yields ($\phi_f$) of ThT at $w$ = 0.5 is 0.046, and in neat EG the quantum yield of ThT is ~0.004. Therefore the quantum yield of ThT increases ~11.5 times in EG containing reverse micelles compared to that in neat EG. With increase in $w$ value $\phi_f$ gradually decreases, at $w$ = 2.0, $\phi_f$ of ThT become 0.02. In isooctane/AOT/Gly reverse micelles the emission quantum yields ($\phi_f$) of ThT at $w$ = 1 is 0.112, and in neat glycerol the quantum yield of ThT is ~0.053. Therefore the quantum yield of ThT increases ~2.1 times in glycerol containing reverse micelles compared to that in neat glycerol. This due to the fact that glycerol is a highly viscous medium, therefore in neat glycerol the quantum yield of ThT is very high compared to methanol or ACN. With increase in $w$ value $\phi_f$ gradually decreases, at $w$ = 3.5, $\phi_f$ of ThT become 0.096.

### 3.2 The effect of viscosity on ThT and determination of microviscosity

We have studied the emission property of ThT in methanol–glycerol mixtures. This mixture of different compositions was used as both the methanol and glycerol have almost same polarity ($E_T(30)$ of glycerol and methanol are 55.4 and 57.0, respectively) and hence the mixtures have almost same polarity, but the mixtures have different viscosity. We found that with gradual increase of viscosity of the mixtures the fluorescence intensity of ThT was gradually increased and the emission spectral position also showed a red shift from 475 nm in methanol to 487 nm in the 90% glycerol of viscosity 630 cP. The quantum yield of the ThT emission in these glycerol–methanol mixtures gradually went on increasing with gradual increase in viscosity, as shown in Table S1 (in ESI†). In solutions of low viscosity the ThT undergoes ultra fast torsional motion along the C–C bond between the two aromatic moieties and this torsional motion opens up the non-radiative decay channel to compete with fluorescence emission and so the fluorescence emission intensity decays to very low in the solutions of low viscosity.[16,17] With gradual increase in viscosity this torsional motion gradually becomes slow and gets retarded and so the non-radiative decay rates become small. Hence fluorescence quantum yield gradually increases. We have plotted the emission quantum yield of ThT against the viscosity of these mixtures using the Förster–Hoffmann equation:[32]

$$\phi_f = Z\eta^{\alpha} \quad (5)$$

where $Z$ and $\alpha$ are the constants and $\eta$ is the viscosity of the medium. The plot of $\phi_f$ *vs.* $\eta$ is used as a calibration curves, as shown in Fig. 4a (the log $\phi_f$ *vs.* log $\eta$ plot is shown in Fig. S-1†). The values of $Z$ and $\alpha$ are $1.8 \times 10^{-4}$ and 0.718, respectively. The value of $\alpha$ matches well with the value ($\alpha$ = 0.5–0.75) reported in the literature for a molecular rotor.[33] From this calibration plot we found out the maximum micro-viscosity faced by ThT in different restricted media. Sulatskaya *et al.*[34] studied the photophysical properties of ThT in glycerol–water mixtures, but here we have used glycerol–methanol mixtures since the polarity of glycerol and methanol are very close to each other. This equation is not valid for the high viscosity region where the radiative relaxation dominates with negligible rotational relaxation.[32,35,36] But in our case we found that the rotational relaxation is not negligible. So we have used eqn (4) to find out the microviscosity faced by ThT in different reverse micelles (Table 3).

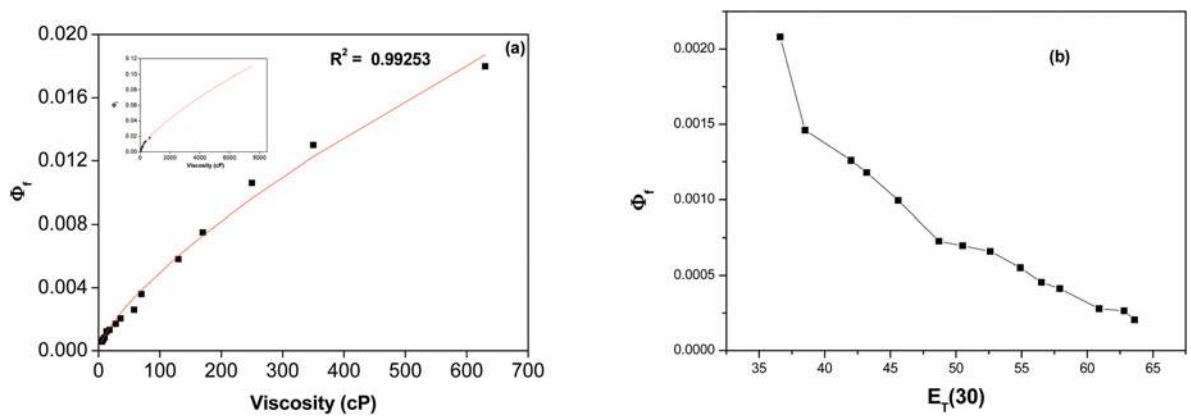


**Fig. 4** (**a**) The calibration curve for determining the microviscosity faced by ThT in different restricted media using glycerol–methanol mixtures of different compositions. (**b**) The variation of the quantum yield of ThT with varying polarity parameter $E_T(30)$ of dioxane–water mixtures.

 

In almost all the reverse micelles, except isooctane/AOT/Gly reverse micelles, with a gradual increase in polar solvent in reverse micelles the fluorescence quantum yield decreases. In the case of isooctane/AOT/Gly reverse micelles addition of glycerol to achieve $w = 1$ causes an increase in the fluorescence quantum yield from that of the $w = 0$ value. After $w = 1$, gradual addition of glycerol causes a decrease in the fluorescence quantum yield. The first increase in the fluorescence quantum yield is mainly due to the increase in microviscosity, which causes the torsional motion of the dye along the C–C bond to be sluggish. So the non-radiative decay rate decreases, which causes the increase in fluorescence quantum yield. Further addition of glycerol beyond the $w = 1$ causes an increase in the size of the reverse micelle and hence greater movement of the ThT molecule towards the polar core from the interface. It is known that in glycerol containing reverse micelles glycerol interacts with AOT through hydrogen bonding with the $SO_3^-$ group of AOT and solvating the $Na^+$ counterion by means of charge–dipole interaction, thereby removing $Na^+$ counterion from the interface[37,38] and disrupting the associated structure of glycerol in these reverse micelles. With increase in $w$ value the ThT molecule shifted to the polar core of the reverse micelles. As a result the microviscosity faced by the ThT gradually decreases with increase in $w$ value and hence the torsional motion of the dye along the C–C bond becomes favourable. From the calibration curve (Fig. 4a) we have found out that the microviscosity faced by ThT in glycerol reverse micelle at $w = 1$ is 7755 cP (Table 3), which is about 2.38 times higher than the microviscosity faced by the probe molecule at $w = 0$. But with a gradual increase in the glycerol content in the reverse micelle this microviscosity faced by ThT gradually decreases. At $w = 3.5$ the microviscosity faced by the ThT is 6257 cP. So this decrease in the microviscosity causes the decrease in the fluorescence quantum yield of ThT. To calculate the radiative and non-radiative decay rate, the following equations are used

$$k_r = \frac{\phi_f}{\tau_f} \quad (6)$$

$$\frac{1}{\tau_f} = k_r + k_{nr} \quad (7)$$

where $\phi_f$ stands for the fluorescence quantum yield of the fluorophore, $\tau_f$ is the fluorescence lifetime, $k_r$ and $k_{nr}$ stand for radiative and non-radiative decay rate constants of the fluorophore. At $w = 1$ the non-radiative decay rate ($k_{nr}$) is $1.39 \times 10^9$ $s^{-1}$ and at $w = 0$ it is $2.03 \times 10^9$ $s^{-1}$. After $w = 1$ further addition of glycerol causes the increase in the non-radiative decay rate constant and at $w = 3.5$ the non-radiative decay rate constant becomes $1.61 \times 10^9$ $s^{-1}$ (Table 1). In glycerol reverse micelles the glycerol molecules inside the polar core of the reverse micelle solvate the $SO_3^-$ head group of AOT, which breaks down their own hydrogen bonding network at lower $w$ value. With gradual increase in the $w$ value the glycerol molecules still solvate the AOT head group. As a result the free glycerol molecules are not present.[37] Addition of more and more glycerol molecules to the core weakens the electrostatic interaction between ThT cations and AOT head groups, thereby decreasing the stability of the ground state of ThT. On the other hand, as more and more glycerol is added, at the same time the ThT molecule is also solvated in the excited state, thereby stabilising the excited state and hence the fluorescence emission peak is red shifted. Ethylene glycol is much less viscous than glycerol. When ethylene glycol is added to the polar core to achieve $w = 0.5$, ethylene glycol molecules enter inside the lipophilic phase and starts to interact with the carbonyl group of AOT.[38] Increase in $w$ value from $w = 0$ to $w = 0.5$ causes the decrease in fluorescence quantum yield to 0.046. Addition of ethylene glycol in the mixture of AOT–isooctane to achieve $w = 0.5$ causes a decrease in the electrostatic interaction between the ThT cation and the polar head group of AOT and the molecule faces less microviscosity, so the torsional motion of the molecule along the C–C bond becomes more favourable and hence the non-radiative decay rate constant gradually increases. As a result of this the fluorescence quantum yield also suffers a decrease to 0.02 at $w = 2$. Again from the steady state data it is observed that the emission peak of ThT undergoes a red shift from 476 nm at $w = 0.5$ to 481 nm at $w = 2$, showing that the ThT molecule is moving towards a more polar region.

In the case of DMF reverse micelles, gradual addition of DMF in the AOT–isooctane mixture causes a decrease in the fluorescence quantum yield. Addition of DMF to the polar core causes the solvation of $Na^+$ ions.[39] Thus there is greater probability that the ThT cation may interact with the polar head group of AOT. This kind of interaction is supported by the fact that the steady state absorption spectra also shows some blue shift with a gradual increase in $w$ value. There is only very small or almost no dipole–dipole interaction between the polar head group of AOT and DMF. The DMF structure inside the pool of the reverse micelle is highly distorted. The quantum yield of ThT in AOT/isooctane/EG reverse micelles at $w = 0.5$ is 0.046 whereas the same in isooctane/AOT/DMF reverse micelles at $w = 0.5$ is 0.058. These data shows that the microenvironment of ThT in DMF containing reverse micelles is different from that of EG containing reverse micelles. With increase in $w$ value ThT molecules move to the polar core of the reverse micelles, facing a less viscous environment, so the non-radiative decay channel opens, leading to the decrease in the fluorescence quantum yield. The fluorescence emission peak also shows a small red shift, indicating that the dye molecule is facing more a polar medium with a gradual increase in $w$ value. Almost the same explanation is applicable for isooctane/AOT/ACN reverse micelles. The special features about ACN and MeOH reverse micelles are that with gradual increase in $w$ value their size does not change much and almost remains the same. In the case of methanol reverse micelles, addition of methanol to the isooctane–AOT mixture to achieve $w = 1$ causes the decrease in fluorescence quantum yield to 0.03 from 0.06 and further addition of methanol to the reverse micelle causes the further decrease in fluorescence quantum yield to 0.003 at $w = 8$. The decrease in fluorescence quantum

yield is probably due to the decrease in the microviscosity. The microviscosity faced by the ThT gradually decreases with gradual increase in the methanol content of the polar pool. Here, viscosity may be the main driving force behind the change of fluorescence quantum yield. We have calculated the value of microviscosity faced by the ThT cation in AOT/isooctane/MeOH reverse micelles and found that microviscosity gradually decreases from 1239 cP at $w = 1$ to 50 cP at $w = 8$. So in methanol reverse micelles the microviscosity faced by the probe decreases ~25 times compared to the 1.24 times decrease in glycerol reverse micelles, proving that inside the reverse micelle no free glycerol molecule exists.

### 3.3 The effect of polarity on ThT

To check whether the emission property of ThT is polarity dependent or not, we studied the fluorescence properties of ThT in dioxane–water mixtures of different composition. With gradual increase of water content in the mixtures the polarity parameter $E_T(30)$ gradually increases from 36.6 (100% dioxane) to 63.6 (100% water).[40–42] It was observed that the absorption peak of ThT shifts from 411 nm in 100% dioxane to 421 nm in a mixture of 81.3% dioxane and further decreases to 412 nm in water. The respective absorption peak positions are tabulated in Table S2 (in ESI†). The structural properties of dioxane–water mixtures are different for different mole fractions of dioxane. Takamuku *et al.*[43] studied the structure and dynamics of 1,4-dioxane–water mixture of different compositions by using X-ray diffraction, mass spectrometry and NMR relaxation. They found that the 1,4-dioxane–water mixtures could be divided into three region: $0.3 \leq X_{diox} \leq 0.9$, $0.1 \leq X_{diox} \leq 0.2$, and $0 \leq X_{diox} \leq 0.07$, where $X_{diox}$ is the mole fraction of dioxane in the mixture. In the region $0.3 \leq X_{diox} \leq 0.9$ the structure of dioxane remains almost unaltered. In the region $0.1 \leq X_{diox} \leq 0.2$ the clusters of one or two molecules of dioxane and several water molecules are formed by means of hydrogen bonding between dioxane and water and still the structure of the water molecules remains ruptured. In this region the hydrogen bonded network of water does not start to be formed. In the region $0 \leq X_{diox} \leq 0.07$ the ice like open network structure starts to predominate and yet the original hydrogen bonded network of water is not formed. This indicates that addition of a small amount of 1,4-dioxane to water causes the break down of the hydrogen bonded water structure. Gradual addition of water to the dioxane causes the formation of free water molecules together with the formation of the dioxane–water cluster, which causes the specific solvation of ThT molecules, causing the red shift of the absorption peak up to 81.3% dioxane in dioxane–water mixture. After the initial red shift of the absorption peak, as the polarity of the medium gradually increases the ground state of the ThT molecule gets more stabilised and so the absorption band shifts further towards the blue end. In pure water the water molecules are associated with each other by means of a hydrogen bonding network and as a small amount of 1,4-dioxane is added to water the hydrogen bonded network of water breaks down and free water molecules are formed together with the formation of dioxane–water cluster. These free water molecules preferentially solvate the ThT, thereby causing the initial red shift of the dye ThT. We found that with gradual increase of polarity *i.e.* gradually increasing proportion of water in the mixtures the fluorescence emission peak showed a shift from 475 nm in 100% dioxane solution to 486 nm up to the dioxane–water mixture having 34.4% dioxane content ($E_T(30) = 56.5$) and then further decreased to 481 nm in water of $E_T(30) = 63.6$ as shown in Table S2 (in ESI†). The absorption and emission energy of ThT in dioxane–water mixtures (in kcal $mol^{-1}$) showed a trend of initial decrease followed by increase. The fluorescence quantum yield of ThT decreases ~10 times on going from neat dioxane to water whereas polarity changed by 27 on the $E_T(30)$ scale (Table S2,† Fig. 4b). From this study it is clear that quantum yield of ThT fluorescence is also dependent on the polarity of the medium. This decrease in quantum yield of ThT with increase in polarity is due to an increase in the rate of TICT. Addition of a small amount of 1,4-dioxane causes the rupture of the hydrogen bonded network of the water molecules and therefore the dioxane molecules remain embedded into the water structure, forming the clathrate hydrate up to the mole fraction of dioxane $X_{diox} \leq 0.1$. Above this mole fraction binary clusters are formed in between 1,4-dioxane and water, containing one or two dioxane molecule and several water molecules and this type of cluster exists in the range $0.1 \leq X_{diox} \leq 0.2$. At the same time there are also several free water molecules, which preferentially solvate the ThT molecule in the excited state and such preferential solvation is responsible for the red shift of the emission maximum. Again further addition of dioxane causes the revival of the neat dioxane cluster and furthermore the decrease of free water molecule in the range of $0.3 \leq X_{diox} \leq 0.9$. As a result the polarity of the medium decreases, causing the blue shift of the emission maximum. Thus the emission maximum of ThT in dioxane is 475 nm. Such kind of preferential solvation also reported in the literature.[44,45] Friedhoff *et al.*[46] also studied the effect of polarity and viscosity on the fluorescence intensity and the emission maxima for ThS and ThT in different solvents and binary solvent mixtures of different polarity and different viscosity. They found that the variation of dielectric constant of the solvents (and hence variation of polarity) caused the spectral intensity change and shift of the spectral peak for ThS, but the polarity change had a negligible effect on the spectral peak position shift in the case of ThT. Sulatskaya *et al.*[33] studied the photophysical properties of ThT in a wide range of viscosity and temperature by incorporating it into the insulin amyloid fibril and rigid isotropic solution. They suggested that the fluorescence quantum yield of ThT not only depended on the ultrafast torsional rotation among the C–C bond between the two fragments but also depended upon the conformation of the dye in both the ground state and also in the excited state and proposed that the non-radiative decay was mainly due to the nonplanar conformation in both the ground state and the excited state. They reported that the fluorescence quantum yield of ThT was not only dependent upon the steric restriction or the ultrafast

 

**Table 2** The fluorescence lifetime values of ThT in different non-aqueous reverse micelles

| No. | System | $\tau_1$ (ns) | $a_1$ | $\tau_2$ (ns) | $a_2$ | $\tau_3$ (ns) | $a_3$ | $\tau_f$ [a] (ns) | $\chi^2$ |
|---|---|---|---|---|---|---|---|---|---|
| 1 | AOT–isooctane mixture | 0.110 | 0.545 | 0.540 | 0.312 | 1.632 | 0.143 | 0.462 | 0.997 |
| 2 | Gly RM at $w$ = 1 | 0.144 | 0.420 | 0.677 | 0.391 | 1.664 | 0.189 | 0.639 | 1.122 |
| 3 | Gly RM at $w$ = 2 | 0.159 | 0.412 | 0.645 | 0.412 | 1.490 | 0.176 | 0.593 | 1.104 |
| 4 | Gly RM at $w$ = 3 | 0.146 | 0.397 | 0.604 | 0.426 | 1.365 | 0.177 | 0.556 | 1.094 |
| 5 | Gly RM at $w$ = 3.5 | 0.146 | 0.382 | 0.586 | 0.426 | 1.328 | 0.192 | 0.560 | 1.122 |
| 6. | EG RM at $w$ = 0.5 | 0.098 | 0.619 | 0.471 | 0.298 | 1.396 | 0.083 | 0.317 | 1.161 |
| 7 | EG RM at $w$ = 1.0 | 0.083 | 0.637 | 0.345 | 0.308 | 0.995 | 0.055 | 0.214 | 1.075 |
| 8 | EG RM at $w$ = 1.5 | 0.072 | 0.646 | 0.274 | 0.312 | 0.820 | 0.042 | 0.166 | 1.124 |
| 9 | EG RM at $w$ = 2.0 | 0.065 | 0.670 | 0.245 | 0.291 | 0.710 | 0.039 | 0.143 | 1.085 |
| 10 | DMF RM at $w$ = 0.5 | 0.100 | 0.626 | 0.500 | 0.289 | 1.490 | 0.085 | 0.334 | 1.130 |
| 11 | DMF RM at $w$ = 1.0 | 0.090 | 0.647 | 0.440 | 0.282 | 1.356 | 0.071 | 0.278 | 1.170 |
| 12 | DMF RM at $w$ = 2.0 | 0.070 | 0.691 | 0.324 | 0.258 | 1.038 | 0.051 | 0.185 | 1.110 |
| 13 | DMF RM at $w$ = 3.0 | 0.060 | 0.752 | 0.262 | 0.220 | 0.846 | 0.028 | 0.126 | 1.189 |
| 14 | ACN RM at $w$ = 1.0 | 0.100 | 0.627 | 0.494 | 0.289 | 1.522 | 0.084 | 0.333 | 1.117 |
| 15 | ACN RM at $w$ = 3.0 | 0.074 | 0.698 | 0.373 | 0.250 | 1.215 | 0.052 | 0.208 | 1.183 |
| 16 | ACN RM at $w$ = 5.0 | 0.060 | 0.741 | 0.096 | 0.222 | 1.018 | 0.037 | 0.103 | 1.196 |
| 17 | MeOH RM at $w$ = 1.0 | 0.092 | 0.667 | 0.452 | 0.264 | 1.396 | 0.069 | 0.277 | 1.120 |
| 18 | MeOH RM at $w$ = 3.0 | 0.050 | 0.808 | 0.240 | 0.168 | 0.855 | 0.024 | 0.101 | 1.071 |
| 19 | MeOH RM at $w$ = 5.0 | 0.036 | 0.878 | 0.180 | 0.115 | 0.686 | 0.007 | 0.057 | 1.092 |
| 20 | MeOH RM at $w$ = 8.0 | 0.030 | 0.941 | 0.165 | 0.057 | 0.755 | 0.002 | 0.040 | 1.128 |

[a] $\langle\tau\rangle = a_1\tau_1 + a_2\tau_2 + a_3\tau_3$. Error: ±5%.

torsional motion along the C–C bond but also on the conformation of the bound dye to the fibril. In our study we observed that the fluorescence quantum yield of ThT is not only dependent on the viscosity of the medium but also dependent on the polarity of the medium.

### 3.4 Time resolved emission study

We have studied the time resolved fluorescence emission spectra of ThT in different reverse micelles (Table 1). All the decays were fitted by a triexponential function (Table 2). Similar multiexponential behaviour of fluorescence lifetime decay of ThT in aqueous reverse micelles has been reported.[15] This multiexponential behaviour observed in the fluorescence decay of ThT in all non-aqueous polar solvents containing reverse micelles is due to heterogeneity of the system. We have taken the average value of fluorescence lifetime of ThT in all the reverse micelles. A similar approach was reported in the literature for several fluorophores in the reverse micelles.[15,22–26,30] In AOT/isooctane/Gly reverse micelles with gradual increase in the $w$ value, the average fluorescence lifetime value first increased from 462 ps at $w$ = 0 to 639 ps at $w$ = 1 and then further decreased to 569 ps at $w$ = 3.5 (Fig. 5a). First increase in the fluorescence average lifetime is due to increase in the viscosity faced by the ThT cation on going from the $w$ = 0 to $w$ = 1. In the case of EG reverse micelles the average fluorescence lifetime of ThT gradually decreases from 317 ps (at $w$ = 0.5) to 143 ps (at $w$ = 2). Gradual increase in EG in the reverse micelle causes the gradual shift of the ThT towards the core of the reverse micelle and hence it faces less viscosity than at the interface. As a result the torsional motion along the C–C bond of ThT becomes more and more favourable. So the average lifetime of ThT gradually decreases (Fig. 5b). Similar trends are also observed in the case of DMF, ACN and MeOH reverse micelles (Fig. 6a, 6b, 6c). In the case of DMF reverse micelles the average fluorescence lifetime of ThT gradually decreases from 334 ps (at $w$ = 0.5) to 126 ps (at $w$ = 2). In the case of ACN reverse micelles the average fluorescence lifetime of ThT gradually decreases from 333 ps (at $w$ = 1.0) to 103 ps (at $w$ = 5). In the case of MeOH reverse micelles the average fluorescence lifetime of ThT gradually decreases from 277 ps (at $w$ = 1.0) to 40 ps (at $w$ = 8). In the case of glycerol reverse micelles the decrease in fluorescence average lifetime of ThT is only 80 ps with increase in $w$ from 1 to 3.5. In the case of EG reverse micelle decrease in fluorescence average lifetime of ThT is 174 ps with increase in $w$ from 0.5 to 2.0.

**Table 3** Microviscosity faced by ThT and torsional rate constants of ThT in different non-aqueous reverse micelles at different $w$ values

| No. | System | Microviscosity in reverse micelles ($\eta$) (cP) | $k_2$ ($\times 10^9$) ($s^{-1}$) | $k_{tor}$ ($\times 10^9$) ($s^{-1}$) |
|---|---|---|---|---|
| 1 | AOT–isooctane mixture | 3252 | 0.323 | 1.716 |
| 2 | Gly RM at $w$ = 1.0 | 7755 | 0.435 | 0.969 |
| 3 | Gly RM at $w$ = 2.0 | 7088 | 0.440 | 1.072 |
| 4 | Gly RM at $w$ = 3.0 | 6257 | 0.430 | 1.187 |
| 5 | Gly RM at $w$ = 3.5 | 6257 | 0.425 | 1.173 |
| 6 | EG RM at $w$ = 0.5 | 2247 | 1.210 | 1.870 |
| 7 | EG RM at $w$ = 1.0 | 1297 | 1.210 | 3.240 |
| 8 | EG RM at $w$ = 1.5 | 908 | 1.202 | 4.597 |
| 9 | EG RM at $w$ = 2.0 | 705 | 1.168 | 5.756 |
| 10 | DMF RM at $w$ = 0.5 | 3102 | 1.365 | 1.615 |
| 11 | DMF RM at $w$ = 1.0 | 2179 | 1.271 | 2.141 |
| 12 | DMF RM at $w$ = 2.0 | 1126 | 1.185 | 3.862 |
| 13 | DMF RM at $w$ = 3.0 | 609 | 1.122 | 6.762 |
| 14 | ACN RM at $w$ = 1.0 | 2112 | 1.092 | 1.742 |
| 15 | ACN RM at $w$ = 3.0 | 961 | 0.992 | 3.481 |
| 16 | ACN RM at $w$ = 5.0 | 516 | 1.282 | 8.374 |
| 17 | MeOH RM at $w$ = 1.0 | 1239 | 3.854 | 1.321 |
| 18 | MeOH RM at $w$ = 3.0 | 268 | 3.533 | 5.597 |
| 19 | MeOH RM at $w$ = 5.0 | 132 | 3.747 | 12.05 |
| 20 | MeOH RM at $w$ = 8.0 | 50 | 2.676 | 22.73 |

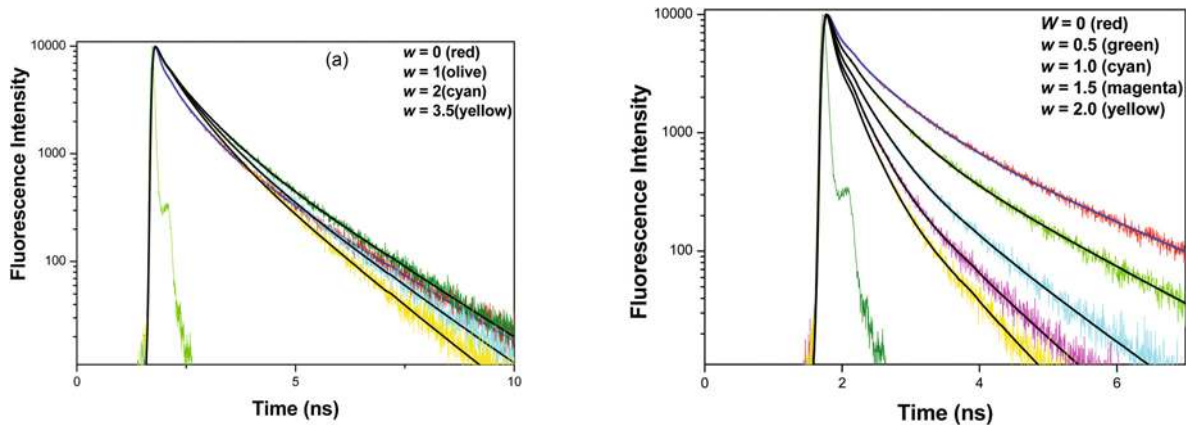


**Fig. 5** The fluorescence lifetime decays for ThT in (**a**) isooctane/AOT/Gly reverse micelles and (**b**) isooctane/AOT/EG reverse micelles at different *w* values.

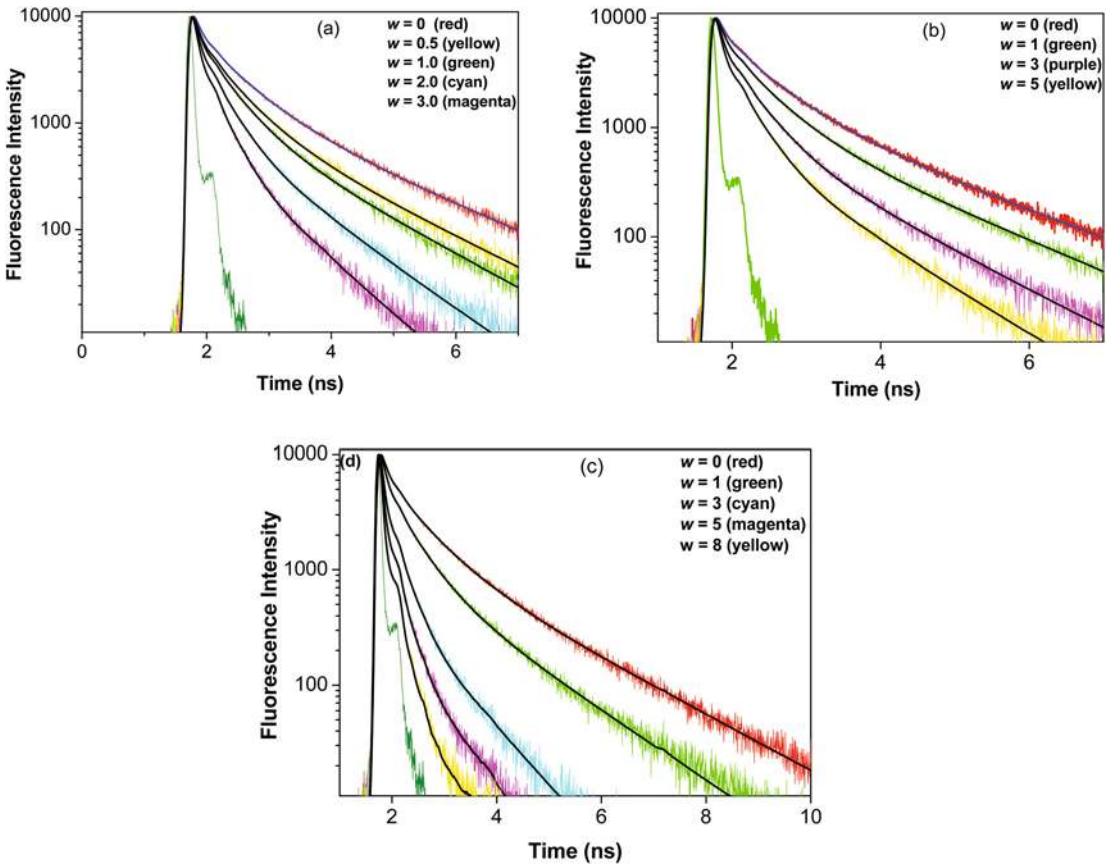


**Fig. 6** The fluorescence lifetime decays for ThT in (**a**) isooctane/AOT/DMF reverse micelles, (**b**) isooctane/AOT/ACN reverse micelles and (**c**) isooctane/AOT/MeOH reverse micelles at different *w* values.

In the case of DMF, ACN and MeOH reverse micelles decrease in the fluorescence average lifetime of ThT are, respectively, 208 ps, 230 ps, 237 ps. So these clearly show that gradual decrease in microviscosity of solvents affects the decrease of excited state lifetime. It is also observed that the non-radiative decay rate decreases more in reverse micelles containing less viscous solvents (MeOH, ACN and DMF) with increasing *w* value than the reverse micelles containing high viscosity solvent (glycerol). The residual for the fitted fluorescence lifetime decay ThT in reverse micelles is shown in the ESI (Fig. S-2†).[64]

### 3.5 Determination of the torsional rate constant of ThT

When a molecule is excited by radiation the molecule goes to the first electronic excited state by means of absorption of radiation. After reaching the excited electronic state the molecule

 

starts to undergo deactivation process by means of several deactivation pathways. These deactivation pathways may be radiative or non-radiative. Non-radiative decays may be due to the internal conversion, which is actually the dissipation of energy of the excited state as heat energy, which is distributed to the ground energy level. This distributed energy further gets distributed among the surrounding medium. Another non-radiative deactivation pathway may be due to the rotational diffusion. Here the surrounding medium also plays an important role in such rotational diffusion. Oster and Nishijima[47] described three types of excited state deactivation pathway, which are as follows:

$$B^* \xrightarrow{k_1} B + h\nu_f (\text{fluorescence}) \quad (i)$$

$$B^* \xrightarrow{k_2} B + \text{heat (all nonradiative processes except torsional motion)} \quad (ii)$$

$$B^* \xrightarrow{k_3} B + \text{heat (nonradiative process only due to rotational diffusion or torsional motion)} \quad (iii)$$

Here we have calculated the radiative rate constant ($k_1$), rate constant of all non-radiative process except torsional motion ($k_2$) and non-radiative decay rate constant due torsional motion ($k_3$). Here B stands for $ThT^+$. The rate constant of the entire process is given by $k = k_1 + k_2 + k_3$. In the absence of any quenching process the rate constant of fluorescence is given by $1/\tau_1$. The fluorescence quantum yield is given by the following equation:

$$\frac{1}{\phi} = 1 + \frac{\tau_1}{\tau_2} + \frac{\tau_1}{\tau_3} \quad (8)$$

Now $k_2 = 1/\tau_2$ and $k_3 = 1/\tau_3$ so the above equation can be written as follows

$$\frac{1}{\phi} = 1 + \frac{k_2}{k_1} + \frac{k_3}{k_1} \quad (9)$$

Now as the rotational diffusion rate constant is dependent upon medium viscosity and the torsional motion is one type of rotational motion, it can be said that $k_{tor} = k_3 \propto T/\eta$ (as the diffusion coefficient is also directly proportional to $T/\eta$). Thus the equation can be modified as follows

$$\frac{1}{\phi} = 1 + \frac{k_2}{k_1} + \frac{aT}{k_1\eta} \quad (10)$$

where $a$ is a proportionality constant.

We have observed a linear correlation between $1/\phi$ and $1/\eta$ (Fig. 7), which indicates that the excited state dynamics of ThT in all non-aqueous reverse micelles are guided by the above processes (i) to (iii). A similar observation was reported by Singh *et al.* on the excited state dynamics of ThT in aqueous reverse micelles.[15] The value of $k_{tor}$ in different reverse micelles are tabulated in Table 3.

### 3.6 Time resolved anisotropy study

We have measured the time resolved fluorescence anisotropy of ThT in different non-aqueous reverse micelles. The time resolved fluorescence anisotropy decay of any probe molecule in micelles or reverse micelles is due to the two different motions and these are the rotational diffusion of the entire dye molecule inside the reverse micelle or micelles and the rotational motion of the entire reverse micelle or micelle. In all reverse micelles, except isooctane/AOT/MeOH reverse micelles, the fluorescence anisotropy was found to increase with an increase in $w$ value (Fig. 8). In the case of Gly, EG and DMF reverse micelles at lower $w$ value fluorescence anisotropy decays were fitted by biexponential functions whereas at higher $w$ value they were fitted by a single exponential function (Table 4). Singh *et al.*[15] observed that the anisotropy value of ThT in aqueous reverse micelles is independent of $w_0$ value. In our case the increase of fluorescence anisotropy value with increase in $w$ appears to be quite contradictory to the usually obtained results. To explain these types of results both hydrodynamic friction and dielectric friction should be considered. The coupling of both hydrodynamic friction and the dielectric friction is responsible for such behaviour. The concept of dielectric friction of a rotating dipole in a polar medium was first treated by Nee and Zwanzig.[48] Later several workers have extensively studied and modified the concept of dielectric friction faced by a solute in polar solvents.[49,50] The dielectric friction mechanism arises due to the specific interaction between the solute (which is considered a point dipole) rotating inside a spherical cavity with the polar medium (considered to be a dielectric continuum) residing outside. This dielectric friction coupled with the hydrodynamic friction is responsible for the increase in the fluorescence anisotropy value and hence the increase in the fluorescence depolarisation time of ThT in reverse micelles. Laia and Costa reported a similar increase in the fluorescence anisotropy of squaraine, with gradual decrease in fluorescence quantum yield with increasing $w$ value.[51] Ferreira and Costa also reported another similar result where the fluorescence anisotropy value increased with gradual decrease in fluorescence quantum yield of R3B in isooctane/AOT/water reverse micelles with increase in $w$ values.[52] Several workers have studied the nature of dielectric friction and showed its application.[53–59] Besides dielectric friction, the rotation of the entire reverse micelle containing the dye can also contribute to the total anisotropy. Valeur and Keh[60] provided the expression showing the dependence of fluorescence anisotropy on both the hydrodynamic volume of the reverse micelle and the rotational relaxation time of the probe molecule inside reverse micelle, which is as follows:

$$\frac{1}{\bar{r}} = \frac{1}{r_0}\left(1 + \frac{RT}{V_h\eta}\tau\right)\left(1 + \frac{3\tau}{\rho_1}\right) \quad (11)$$

where $V_h$ is the hydrodynamic volume of the reverse micelles, $\rho_1$ is the internal rotational relaxation time of the probe and $\bar{r}$ is the mean anisotropy. So in reverse micelles the average anisotropy depends on both the rotational diffusion of the

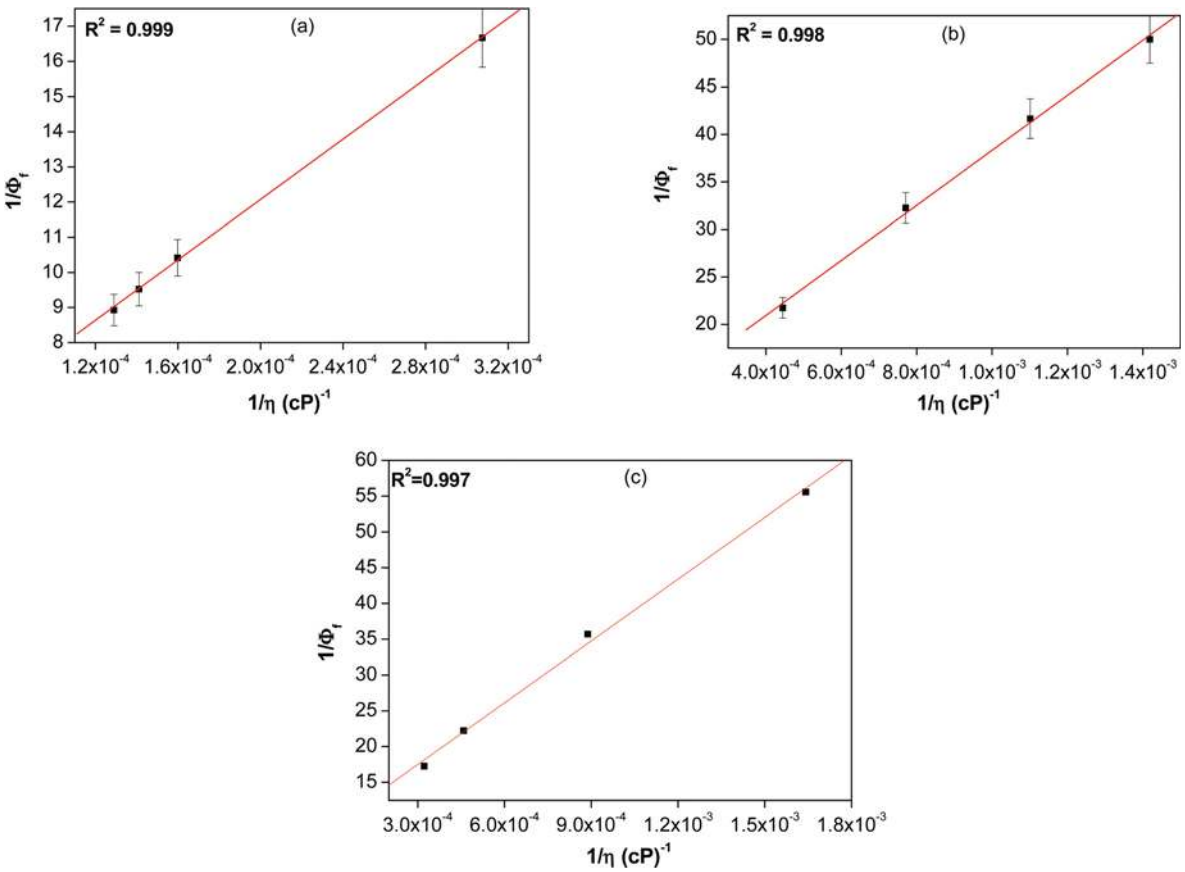


**Fig. 7** The plot of $1/\phi_f$ against the $1/\eta$ value for ThT in (**a**) isooctane/AOT/Gly reverse micelles, (**b**) isooctane/AOT/EG reverse micelles and (**c**) isooctane/AOT/DMF reverse micelles of different $w$ values to obtain different non-radiative rate constants.

micelles and the internal rotational diffusion of the probe molecules. It was reported in the literature that fluorescence depolarisation in the micellar medium was mainly due to the rotational diffusion of the probe molecule inside the micelle, the rotation of the entire micelle and the translational diffusion of the probe molecule along the micelle surface.[61–63] The radius of the isooctane/AOT/Gly reverse micelle can be estimated from the relation:[51] $r_h$/Å = 15 + 9$w$. The radius of the isooctane/AOT/EG reverse micelle at $w$ = 1.5 and 2 is 21.7 and 28.5 Å, respectively.[21] The average rotational relaxation time of ThT in AOT/isooctane/Gly reverse micelles at $w$ = 1 and 3.5 are 5.77 and 8.11 ns, respectively. The average rotational relaxation time of ThT in AOT/isooctane/EG reverse micelles at $w$ = 0.5 and 2 are 2.37 and 5.35 ns, respectively. In the case of Gly and EG reverse micelles, with increase in the size of the reverse micelles the rotational relaxation of the entire reverse micelles also becomes slow. This can also contribute to the increase in the rotational relaxation time and anisotropy in the case of glycerol and ethylene glycol reverse micelles. The diameter of the isooctane/AOT/DMF reverse micelles at $w$ = 1 is ~4 nm.[64] The average rotational relaxation time of ThT in isooctane/AOT/DMF reverse micelles at $w$ = 1 and 3 are 2.28 and 2.80 ns, respectively. The diameter of the isooctane/AOT/ACN and isooctane/AOT/MeOH reverse micelles remains almost same with increase in $w$ value.[65] The diameters of these reverse micelles are ~3 nm.[65] The average rotational relaxation time of ThT in isooctane/AOT/ACN reverse micelles at $w$ = 1 and 5 is 1.89 and 2.30 ns, respectively. The average rotational relaxation time of ThT isooctane/AOT/MeOH reverse micelles at $w$ = 1 is 1.74 ns. We were not able to fit the fluorescence anisotropy of ThT in isooctane/AOT/MeOH reverse micelles at $w$ = 8. Fitting data showed a component of 10 ps with high $\chi^2$ value. This data is not reliable due to limited time resolution of our set up (FWHM = 75 ps).

## 4. Conclusion

We found that the spectral behaviour of the cationic dye ThT is largely viscosity dependent and also at the same time depends upon polarity. We have studied the photophysical properties of ThT in Gly, EG, DMF, ACN, MeOH reverse micelles. We found that in the case of glycerol containing reverse micelles the fluorescence quantum yield first increased on addition of the glycerol in AOT–isooctane mixture and then further decreased with further increase in $w$ value. The average fluorescence lifetime value showed a similar trend. In the case of other non-aqueous reverse micelles (EG, DMF, ACN, MeOH) the fluorescence quantum yields as well as the average fluorescence lifetime decreased in a regular pattern. We considered

 

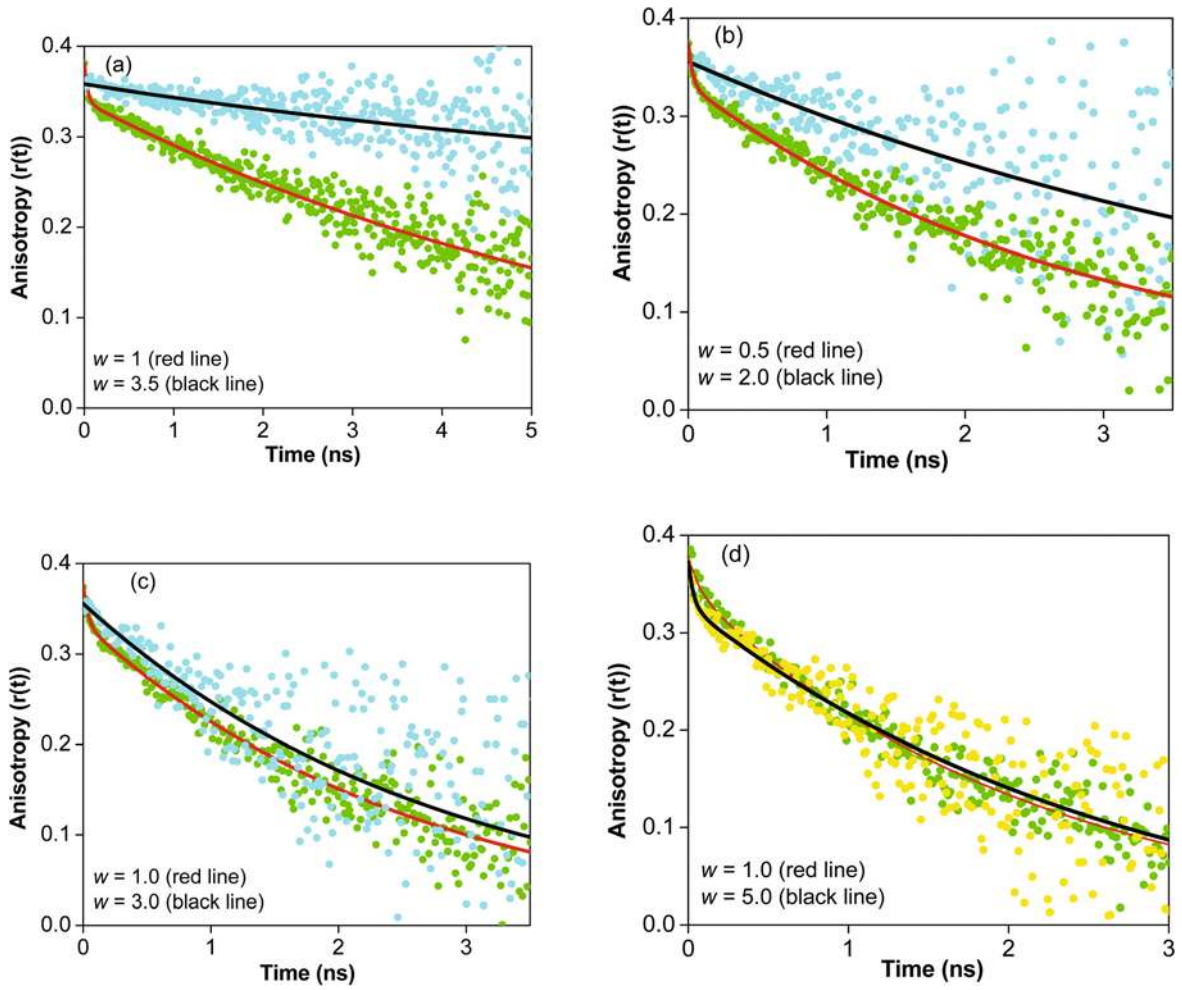


**Fig. 8** The anisotropy decays of ThT in different non-aqueous reverse micelles at different *w* values, (**a**) isooctane/AOT/Gly reverse micelle, (**b**) isooctane/AOT/EG reverse micelle, (**c**) isooctane/AOT/DMF reverse micelle and (**d**) isooctane/AOT/ACN reverse micelle.

**Table 4** The rotational relaxation times of ThT in reverse micelles (RM)

| No. | System | *w* | $\tau_1$ (ns) | $a_1$ | $\tau_2$ (ns) | $a_2$ | $\langle\tau\rangle_{rot}$ [a] (ns) | $\chi^2$ |
|---|---|---|---|---|---|---|---|---|
| 1 | ThT in AOT/isooctane/Gly RM | 1 | 0.040 | 0.14 | 6.71 | 0.86 | 5.77 | 0.96 |
| 2 | | 3.5 | — | — | 8.81 | 1 | 8.81 | 0.99 |
| 3 | ThT in AOT/isooctane/EG RM | 0.5 | 0.030 | 0.17 | 2.86 | 0.83 | 2.37 | 1.04 |
| 4 | | 2.0 | — | — | 5.35 | 1 | 5.35 | 1.00 |
| 5 | ThT in AOT/isooctane/DMF RM | 1 | 0.04 | 0.14 | 2.64 | 0.86 | 2.28 | 1.0 |
| 6 | | 3 | — | — | 2.80 | 1.0 | 2.80 | 0.99 |
| 7 | ThT in AOT/isooctane/Methanol RM | 1 | 0.035 | 0.12 | 1.97 | 0.88 | 1.74 | 1.03 |
| 8 | ThT in AOT/isooctane/ACN RM | 1 | 0.065 | 0.10 | 2.10 | 0.90 | 1.89 | 1.11 |
| 9 | | 5 | 0.035 | 0.15 | 2.70 | 0.85 | 2.30 | 0.99 |

[a] $\langle\tau\rangle_{rot} = a_1\tau_1 + a_2\tau_2$.

that with gradual increase in *w* value the probe molecule experienced a less viscous environment and hence a gradual decrease in fluorescence quantum yield. We constructed a calibration curve by plotting the fluorescence quantum yield against the viscosity by studying the fluorescence emission properties of ThT in glycerol–methanol mixtures. From that calibration curve we deduced the microviscosity faced by the ThT in the above-mentioned non-aqueous reverse micelles of different *w* values. We also studied the fluorescence emission and steady state absorption spectral behaviour of ThT in dioxane–water mixtures to observe the effect of polarity on the change of fluorescence quantum yield and found that increase

in polarity caused the decrease in the fluorescence quantum yield. We have observed changes in emission peak position with changes in polarity. The effect of polarity on the change of the fluorescence quantum yield cannot be neglected. The fluorescence anisotropy values in the case of Gly, EG, DMF and ACN reverse micelles showed an increase with increase of $w$ value. We predicted that the dielectric friction coupled with hydrodynamic friction may be responsible for the increase of anisotropy in the reverses micelles. This increase in anisotropy may be also due to rotation of the entire reverse micelles.

## Acknowledgements

D. S. is thankful to IIT Patna, India for research facilities. A. C. is thankful to IIT Patna and CSIR, New Delhi for a research fellowship. We are thankful to reviewers for their constructive comments and suggestions.

## References

1 A. A. Maskevich, V. I. Stsiapura, V. A. Kuzmitsky, I. M. Kuznetsova, O. I. Povarova, V. N. Uversky and K. K. Turoverov, *J. Proteome Res.*, 2007, **6**, 1392.
2 R. Sabate and S. J. Saupe, *Biochem. Biophys. Res. Commun.*, 2007, **360**, 135.
3 L. R. Naika, A. B. Naika and H. Pal, *J. Photochem. Photobiol., A*, 2009, **204**, 161.
4 V. I. Stsiapura, A. A. Maskevich, S. A. Tikhomirov and O. V. Buganov, *J. Phys. Chem. A*, 2010, **114**, 8345.
5 M. Groenning, *J. Chem. Biol.*, 2010, **3**, 1.
6 C. C. Kitts and D. A. V. Bout, *J. Phys. Chem. B*, 2009, **113**, 12090.
7 M. Groenning, M. Norrman, J. M. Flink, M. van de Weert, J. T. Bukrinsky, G. Schluckebier and S. Frokjaer, *J. Struct. Biol.*, 2007, **159**, 483.
8 R. Khurana, C. Coleman, C. I. Zanetti, S. A. Carter, V. Krishna, R. K. Grover, R. Roy and S. Singh, *J. Struct. Biol.*, 2005, **151**, 229.
9 R. Sabate, I. Lascu and S. J. Saupe, *J. Struct. Biol.*, 2008, **162**, 387.
10 P. K. Singh, M. Kumbhakar, H. Pal and S. Nath, *J. Phys. Chem. B*, 2010, **114**, 5920.
11 C. R. Raj and R. Ramaraj, *Chem. Phys. Lett.*, 1997, **273**, 285.
12 M. Ilanchelian and R. Ramaraj, *J. Photochem. Photobiol., A*, 2004, **162**, 129.
13 J. Mohanty, S. D. Choudhury, H. P. Upadhyaya, A. C. Bhasikuttan and H. Pal, *Chem.–Eur. J.*, 2009, **15**, 5215.
14 S. Kumar, A. K. Singh, G. Krishnamoorthy and R. Swaminathan, *J. Fluoresc.*, 2008, **18**, 1199.
15 P. K. Singh, M. Kumbhakar, H. Pal and S. Nath, *J. Phys. Chem. B*, 2009, **113**, 8532.
16 V. I. Stsiapura, A. A. Maskevich, V. A. Kuzmitsky, K. K. Turoverov and I. M. Kuznetsova, *J. Phys. Chem. A*, 2007, **111**, 4829.
17 V. I. Stsiapura, A. A. Maskevich, V. A. Kuzmitsky, V. N. Uversky, I. M. Kuznetsova and K. K. Turoverov, *J. Phys. Chem. B*, 2008, **112**, 15893.
18 N. Amdursky, R. Gepshtein, Y. Erez and D. Huppert, *J. Phys. Chem. A*, 2011, **115**, 8479.
19 E. Friberg and M. Podzimek, *Colloid Polym. Sci.*, 1984, **262**, 252.
20 R. D. Falcone, N. M. Correa, M. A. Biasutti and J. J. Silber, *Langmuir*, 2000, **16**, 3070.
21 C. A. T. Laia, P. Lopez-Cornejo, S. M. B. Costa, J. d'Oliveira and J. M. G. Martinho, *Langmuir*, 1998, **14**, 3531.
22 H. Shirota and K. Horie, *J. Phys. Chem. B*, 1999, **103**, 1437.
23 P. Hazra and N. Sarkar, *Chem. Phys. Lett.*, 2001, **342**, 303.
24 P. Hazra, D. Chakrabarty and N. Sarkar, *Chem. Phys. Lett.*, 2002, **358**, 523.
25 P. Hazra, D. Chakrabarty and N. Sarkar, *Langmuir*, 2002, **18**, 7872.
26 P. Hazra, D. Chakrabarty and N. Sarkar, *Chem. Phys. Lett.*, 2003, **371**, 553.
27 A. I. Sulatskaya, I. M. Kuznetsova and K. K. Turoverov, *J. Phys. Chem. B*, 2011, **115**, 11519.
28 G. Jones II, W. R. Jackson, C.-y Choi and W. R. Bergmark, *J. Phys. Chem.*, 1985, **89**, 294.
29 E. S. Voropai, M. P. Samtsov, K. N. Kaplevskii, A. A. Maskevich, V. I. Stepuro, O. I. Povarova, I. M. Kuznetsova, K. K. Turoverov, A. L. Fink and V. N. Uverskiid, *J. Appl. Spectrosc.*, 2003, **70**, 868.
30 C. Ghatak, V. G. Rao, R. Pramanik, S. Sarkar and N. Sarkar, *J. Phys. Chem. B*, 2011, **115**, 6644.
31 P. Setua, D. Seth and N. Sarkar, *Phys. Chem. Chem. Phys.*, 2009, **11**, 8913.
32 T. Förster and G. Hoffmann, *Z. Phys. Chem.*, 1971, **75**, 63.
33 J. A. Levitt, P. H. Chung, M. K. Kuimova, G. Yahioglu, Y. Wang, J. Qu and K. Suhling, *ChemPhysChem*, 2011, **12**, 662.
34 A. I. Sulatskaya, A. A. Maskevich, I. M. Kuznetsova, V. N. Uversky and K. K. Turoverov, *PLoS One*, 2010, **5**, e15385.
35 M. A. Haidekker and E. A. Theodorakis, *J. Biol. Eng.*, 2010, **4**, 11.
36 S. K. Saha, P. Purkayasthaa, A. B. Das and S. Dhara, *J. Photochem. Photobiol., A*, 2008, **199**, 179.
37 A. M. Durantini, R. D. Falcone, J. J. Silber and N. M. Correa, *J. Phys. Chem. B*, 2011, **115**, 5894.
38 R. D. Falcone, J. J. Silber, M. A. Biasutti and N. M. Correa, *ARKIVOC*, 2011 (vii), 369.
39 R. D. Falcone, N. M. Correa, M. A. Biasutti and J. J. Silber, *J. Colloid Interface Sci.*, 2006, **296**, 356.
40 C. Reichardt, *Chem. Rev.*, 1994, **94**, 2319.
41 E. M. Kosower and H. Dodiuk, *J. Am. Chem. Soc.*, 1978, **100**, 4173.
42 D. Seth, S. Sarkar, R. Pramanik, C. Ghatak, P. Setua and N. Sarkar, *J. Phys. Chem. B*, 2009, **113**, 6826.
43 T. Takamuku, A. Yamaguchi, M. Tabata, N. Nishi, K. Yoshida, H. Wakita and T. Yamaguchi, *J. Mol. Liq.*, 1999, **83**, 163.

 

44 M. Panigrahi, S. Dash, S. Patel and B. K. Mishra, *J. Phys. Chem. B*, 2011, **115**, 99.
45 T. Pradhan, P. Ghoshal and R. Biswas, *J. Phys. Chem. A*, 2008, **112**, 915.
46 P. Friedhoff, A. Schneider, E. M. Mandelkow and E. Mandelkow, *Biochemistry*, 1998, **37**, 10223.
47 G. Oster and Y. Nishijima, *J. Am. Chem. Soc.*, 1956, **78**, 1581.
48 T. W. Nee and R. Zwanzig, *J. Chem. Phys.*, 1970, **52**, 6353.
49 M. G. Kurnikova, D. H. Waldeck and R. D. Coalson, *J. Chem. Phys.*, 1996, **105**, 628.
50 N. Balabai, A. Sukharevsky, I. Read, B. Strazisar, M. Kurnikova, R. S. Hartman, R. D. Coalson and D. H. Waldeck, *J. Mol. Liq.*, 1998, **77**, 37.
51 C. A. T. Laia and S. M. B. Costa, *Langmuir*, 2002, **18**, 1494.
52 J. A. B. Ferreira and S. M. B. Costa, *J. Phys. Chem. B*, 2010, **114**, 10417.
53 M. Choi, D. Jin, H. Kim, T. J. Kang, S. C. Jeoung and D. Kim, *J. Phys. Chem. B*, 1997, **101**, 8092.
54 S. Kuehn, J. A. Marohn and R. F. Loring, *J. Phys. Chem. B*, 2006, **110**, 14525.
55 R. Biswas and B. Bagchi, *J. Am. Chem. Soc.*, 1997, **119**, 5946.
56 R. Biswas, N. Rohman, T. Pradhan and R. Buchner, *J. Phys. Chem. B*, 2008, **112**, 9379.
57 M. L. Horng, J. A. Gardecki and M. Maroncelli, *J. Phys. Chem. A*, 1997, **101**, 1030.
58 R. P. Matthews, G. A. Venter and K. J. Naidoo, *J. Phys. Chem. B*, 2011, **115**, 1045.
59 K. Wiemers and J. F. Kauffman, *J. Phys. Chem. A*, 2000, **104**, 451.
60 E. Keh and B. Valeur, *J. Colloid Interface Sci.*, 1981, **79**, 465.
61 F. L. Quitevis, A. H. Marcus and M. D. Fayer, *J. Phys. Chem.*, 1993, **97**, 5762.
62 N. C. Maiti, S. Mazumdar and N. Periasamy, *J. Phys. Chem.*, 1995, **99**, 10708.
63 G. B. Dutt, *J. Phys. Chem. B*, 2003, **107**, 10546.
64 H. Shirota and H. Segawa, *Langmuir*, 2004, **20**, 329.
65 R. E. Riter, J. R. Kimmel, E. P. Undiks and N. E. Levinger, *J. Phys. Chem. B*, 1997, **101**, 8292.